2004

A missense mutation in the γD crystallin gene (CRYGD) associated with autosomal dominant "coral-like" cataract linked to chromosome 2q

Donna S. Mackay
Washington University School of Medicine in St. Louis

Usha P. Andley
Washington University School of Medicine in St. Louis

Alan Shiels
Washington University School of Medicine in St. Louis

Molecular Vision 2004; 10:155-62 <http://www.molvis.org/molvis/v10/a21>
Received 2 February 2004 | Accepted 16 March 2004 | Published 17 March 2004

A missense mutation in the γD crystallin gene (*CRYGD*) associated with autosomal dominant "coral-like" cataract linked to chromosome 2q

Donna S. Mackay,[1] Usha P. Andley,[1,2] Alan Shiels[1,3]

Departments of [1]Ophthalmology & Visual Sciences, [2]Biochemistry & Molecular Biophysics, and [3]Genetics, Washington University School of Medicine, St. Louis, MO

Purpose: Hereditary cataract is a clinically and genetically heterogeneous lens disorder that usually presents as a sight-threatening trait in childhood. The purpose of this study was to map and identify the mutation underlying an autosomal dominant form of coral-shaped cataract segregating in a three generation Caucasian pedigree.
Methods: Genomic DNA was prepared from blood leucocytes, genotyping was performed using microsatellite markers, and LOD scores were calculated using the LINKAGE programs. Mutation detection was performed using direct sequencing and primer extension analysis. Following site-directed mutagenesis, mutant and wild type expression constructs were transfected into a human lens epithelial cell line (HLE B-3) and recombinant protein was detected by immunoblotting, imunofluorescence, and immunogold microscopy. Cell death was monitored by fluorescence activated cell sorting.
Results: Significant evidence of linkage was detected at markers D2S371 (LOD score [Z]=3.81, recombination fraction [θ]=0) and D2S369 (Z=3.64, θ=0). Haplotyping indicated that the disease gene lay in the approximate 10 Mb physical interval between D2S1384 and D2S128, containing the γ-crystallin gene (*CRYGA-CRYGD*) cluster on chromosome 2q33.3-q34. Sequencing of the *CRYGA-CRYGD* cluster identified a C->A transversion in exon 2 of *CRYGD* that was predicted to result in the non-conservative substitution of threonine for proline at amino-acid residue 23 (P23T) in the processed CRYGD protein. Transfection studies suggested that the P23T mutant was less soluble than its wild type counterpart when expressed in HLE B-3 cells.
Conclusions: This study has identified an eighth type of cataract morphology associated with *CRYGD* and suggests that a *CRYGD* mutation may underlie the historically important "coralliform" cataract first reported in 1895.

At least eleven crystallin genes encode over 95% of the water-soluble structural proteins present in the crystalline lens [1], representing >30% of its mass [2], and accounting for its optical transparency [3] and high refractive index [4,5]. These genes may be divided into two distinct evolutionary groups comprising two α-crystallins (*CRYAA* and *CRYAB*), which are members of the small heat shock family of molecular chaperones, and nine β-/γ-crystallins (*CRYBA1/A3/A4/B1/B2/B3* and *CRYGC/D/S*) which share a common two-domain structure composed of Greek-key motifs, and belong to the family of epidermis-specific differentiation proteins [2]. Because of their abundant expression in the lens, crystallin genes represent compelling candidates for certain hereditary forms of lens opacity, or cataract, that usually present at birth (congenital) or during infancy and which represent a clinically significant cause of vision impairment in childhood [6].

Presently, Online Mendelian Inheritance in Man lists at least sixteen mutations affecting eight human crystallin genes that have been associated with non-syndromic forms of Mendelian cataract, most often exhibiting autosomal dominant transmission. Clinical descriptions of these crystallin-related cataracts have revealed considerable interfamilial variation with respect to the physical location and appearance of opacities in different developmental regions of the juvenile lens [7,8]. Thus, missense and nonsense mutations in *CRYAA* on 21q have been linked with central nuclear cataract [9,10] and autosomal recessive cataract [11], and a deletion mutation in *CRYAB* on 11q underlies posterior polar cataract [12]. A splice-site mutation in *CRYBA3/A1* on 17q has been associated with sutural cataract [13-15], whereas nonsense mutations in *CRYBB1* and *CRYBB2* on 22q have been linked with pulverulent cataract [16,17], cerulean cataract [18], and sutural cataract [19]. Finally, insertion and missense mutations in *CRYGC* on 2q have been linked with zonular pulverulent cataract [20,21] and lamellar cataract [22], whereas, missense and nonsense mutations in neighboring *CRYGD* underlie aculeiform cataract [20,23], crystal cataract [24], progressive punctate cataract [25], lamellar and central nuclear cataract [22], cerulean cataract [26,27], and flaky, silica-like nuclear cataract [15].

To gain further insights about the relationship between crystallin gene mutations and cataract morphology, we have carried out linkage analysis in a family segregating autosomal dominant coral-like cataract and subsequently identified a missense mutation in *CRYGD*.

Correspondence to: Alan Shiels, Ph.D., Ophthalmology and Visual Sciences, Box 8096, Washington University School of Medicine, 660 South Euclid Avenue, St. Louis, MO, 63110; Phone: (314) 362-1637; FAX: (314) 362-3131; email: shiels@vision.wustl.edu

METHODS

Genotyping and linkage analysis: Genomic DNA was extracted from peripheral blood leukocytes using the QIAamp DNA blood maxi kit (Qiagen, Valencia, CA) and Généthon microsatellite $(CA)_n$ repeat markers [28] were amplified using the polymerase chain reaction (PCR) and detected using a Li-Cor 4200 DNA analyzer running Gene ImageR software (Li-Cor, Lincoln, NE) as described previously [10]. Pedigree and haploptype data were managed using Cyrillic (version 2.1) software (FamilyGenetix Ltd., Reading, United Kingdom) and two point LOD scores (Z) calculated using the MLINK subprogram from the LINKAGE (version 5.1) package of programs [29]. Microsatellite marker allele frequencies used for linkage analysis were those calculated by Généthon [28]. A gene frequency of 0.0001 and a penetrance of 100% were assumed for the cataract locus.

Mutation analysis: Exon/intron boundaries in *CRYGA-CRYGD* were identified using the Ensembl human genome browser. Gene-specific PCR primers (Table 1) were designed to anneal to intronic sequence flanking exon boundaries. Genomic DNA was PCR amplified, purified and direct sequenced using dye-terminator chemistry as described previously [10]. Primer extension analysis was performed using wild type and mutant allele-specific primers (Table 1) and the resulting PCR products separated and visualized in 2% agarose gels containing 0.05% ethidium bromide. In order to distinguish the predicted mutation, with 95% confidence, from a polymorphism with 1% frequency we carried out primer extension analysis or direct sequencing of genomic DNA samples from a panel of 170 unrelated control individuals as recommended previously [30].

Expression construct and site-directed mutagenesis: Total RNA was isolated from human postmortem lenses using Trizol (Invitrogen, Carlsbad, CA) and cDNA was reverse transcribed in the presence of random hexamers then amplified using the GeneAmp RNA PCR kit (Roche, Indianapolis, IN) and the following *CRYGD*-specific primers flanking the translation start (ATG) and stop (TGA) codons; sense 5'-GCC ACC ATG GGG AAG ATC ACC CTC TAC G and anti-sense 5'-TTA TCA GGA ATC TAT GAC TCT CCT CAG. The resulting wild type CRYGD coding sequence (528 bp) was subcloned into the pcDNA3.1 mammalian expression vector (Invitrogen) and verified by sequencing using the T7 sequencing primer. Site-directed mutagenesis of wild type *CRYGD* was performed using the QuikChange Mutagenesis kit (Stratagene, La Jolla, CA) and verified by sequencing prior to transfection. Sequences of the complementary sense and antisense primers used to introduce the C->A mutation at the first nucleotide of codon 24 were; 5'-TGC AGC AGC GAC CAC ACC AAC CTG CAG CCC and 5'-GGG CTG CAG GTT GGT GTG GTC GCT GCT GCA, respectively.

Cell culture and transfection: Human lens epithelial cells with extended life span (HLE B-3) were cultured, transfected, selected, and expanded as described previously [31-33].

Immunoblot analysis: Quantitative immunoblot analysis was performed as described previously [32,34] using an antiserum (diluted 1:1,000) raised against bovine γ-crystallins [35]

Table 1. PCR primers for mutation screening of *CRYGA-CRYGD* on 2q

Gene (Exon)	Strand	Sequence (5'-3')
CRYGA (1-2)	Sense	TCCCTTTTGTGTTGTTTTTGCC
	Antisense	TATGGCCATGGATCATTGATGC
CRYGA (3)	Sense	TCGTTGACACCCAAGGATGCATGC
	Antisense	TACAAGAGCCACTTAGTGCAGGG
CRYGB (1-2)	Sense	TGCAAATCCCCTACTCACCAAAATGG
	Antisense	TAAAAGATGGAAGGCAAAGACAGAGCC
CRYGB (3)	Sense	TAGGGACTGGAGCTTTAATTTCC
	Antisense	TACTAGTGCCAGAAACACAAGC
CRYGC (1-2)	Sense	TGCAGGATGTTAAGAGATGC
	Antisense	TTCTCTGATGTCCATCTAAGC
CRYGC (3)	Sense	TATTCCATGCCACAACCTACC
	Antisense	TTGACAGAAGTCAGCAATTGC
CRYGD (1-2)	Sense	TCTTTTGTGCGGTTCTTGCCAACG
	Antisense	TACCATCCAGTGAGTGTCCTGAGG
	Mutant	TCAAGTAGGGCTGCAGGTTGGT
CRYGD (3)	Sense	TCTTTTTATTTCTGGGTCCGCC
	Antisense	TACAAGCAAATCAGTGCCAGG

Primer pairs used for amplification and sequencing of exons from the *CRYGA-CRYGD* gene cluster located on chromosome 2q.

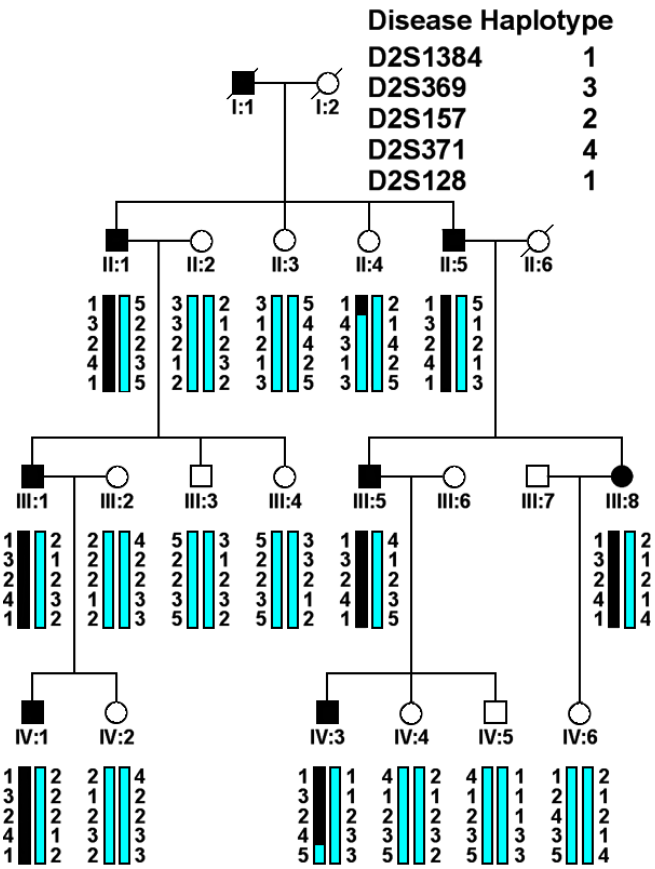

Figure 1. Pedigree and haplotype analysis of the cataract family. Four-generation pedigree segregating autosomal dominant coral-like cataract. Haplotyping shows segregation of five microsatellite markers on 2q listed in descending order from the centromere. Squares and circles symbolize males and females respectively. Blackened symbols and bars denote afffected status.

and horseradish peroxidase-labelled goat-ant-rabbit IgG, then detected by chemiluminescence using Luminol reagent (Santa Cruz Biotechnology, Santa Cruz, CA) and X-ray film (Eastman Kodak Co., Rochester, NY). Blots were re-probed with beta-tubulin antibody (Sigma, St. Louis, MO) to confirm equal loading of samples.

Immunofluorescence microscopy: Transfected cells were fixed, permeabilized and immunostained with γ-crystallin antiserum (1:5,000) followed by an Alexa488-conjugated goat anti-rabbit IgG (Molecular Probes, Eugene, OR) and Texas Red-phalloidin (Molecular Probes) as described previously [34] then viewed under a confocal microscope (Zeiss LSM 510, Thornwood, NY).

Cryo-immunoelectron microscopy: Transfected cells were fixed, embedded, cryo-preserved, sectioned and incubated with γ-crystallin antiserum (1:5,000) followed by goat anti-mouse IgG conjugated with 18 nm gold particles (Sigma), then stained and viewed under a transmission electron microscope (JEOL1200EX, Peabody, MA) as described previously [10].

Fluorescence activated cell sorting (FACS) analysis: Transfected cells were labeled with Annexin V-FITC and propidium iodide (Pharmingen, San Diego, CA), and the percentage of apoptotic cells quantified by flow cytometry using a FACScan running CellQuest software (Becton Dickinson, San Jose, CA) as described previously [33].

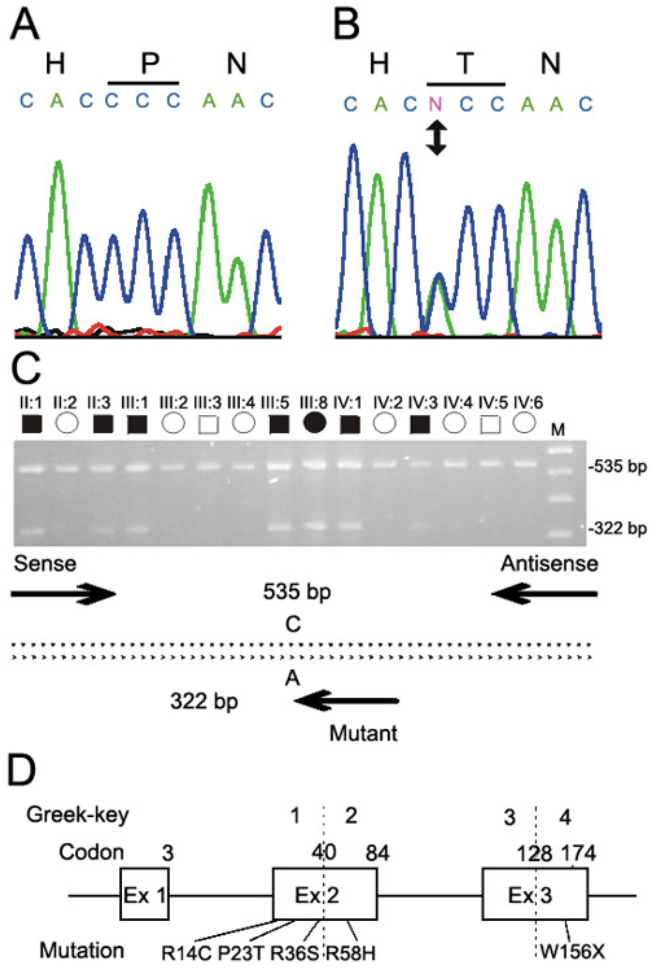

RESULTS

Linkage analysis: We ascertained a three-generation Caucasian family segregating autosomal dominant cataract in the absence of other ocular or systemic abnormalities (Figure 1). No clinical photographs of the lens opacities were available, however, ophthalmic records indicated that the bilateral cataract presented during infancy and was described as coralliform or axial [36-38], having long trumpet-shaped opacities grouped toward the center of the lens and projecting radially forward resembling a piece of coral. This study was approved by the institutional review board at Washington University School of Medicine and all participants provided informed consent prior to enrollment.

Seventeen members of the family including seven affected individuals, eight unaffected individuals, and two spouses were genotyped with microsatellite markers [28] at five crystallin loci linked with autosomal dominant cataract on 2q, 11q, 17q, 21q, and 22q. Following exclusion of four of these loci, we obtained significant evidence of linkage (Table 2) for markers D2S371 (Z=3.81, θ=0) and D2S369 (Z=3.64, θ= 0) on 2q33.3-q34.

Haplotyping of the pedigree (Figure 1) detected one affected male (IV:3) and one unaffected female (II:4) who were obligate recombinants at D2S128 and at D2S1384, respectively. However, no recombinant individuals were detected at

Table 2. Two-point LOD scores for linkage between the cataract locus and 2q markers

		Z at θ=							
Marker	Mb	0.00	0.05	0.1	0.2	0.3	0.4	Z(max)	θ(max)
D2S1384	205.2	-∞	1.87	1.89	1.59	1.10	0.51	1.91	0.08
D2S369	207.4	3.64	3.31	2.96	2.20	1.37	0.53	3.64	0.00
D2S157	211.1	0.60	0.54	0.47	0.32	0.17	0.05	0.60	0.00
D2S371	212.3	3.81	3.47	3.12	2.37	1.53	0.66	3.81	0.00
D2S128	215.0	-0.86	2.22	2.20	1.78	1.17	0.50	2.24	0.07
D2S2248	217.9	-∞	-0.56	0.07	0.38	0.28	0.05	0.38	0.21

Two point LOD scores (Z) for linkage between the cataract locus and six markers on 2q listed in physical order from 2p-tel, measured in megabases (Mb). In the table, Z_{max} and θ_{max} are denoted by Z(max) and θ(max), respectively.

Figure 2. Mutation analysis of *CRYGD.* Sequence chromatograms of the wild type allele (**A**) showing translation of proline (CCC) and the mutant allele (**B**) showing a C->A transversion that substituted threonine (ACC) for proline at amino-acid position 23 (P23T). **C**: Agarose-gel electrophoresis of allele-specific primer extension products generated using the three PCR primers (Table 1) indicated by arrows in the schematic diagram; the sense anchor primer was located in the 5'-upstream region, the antisense primer was located in intron 2 and the nested mutant primer was specific for the A-allele. Unaffected relatives are homozygous for the wild type C-allele (535 bp), whereas, affected relatives are heterozygous for the mutant A-allele (322 bp). The letter M designates a 100 bp size ladder. **D**: Exon organization and mutation profile of *CRYGD*. Codons and corresponding Greek-key protein domains are numbered above each exon. The relative locations of the P23T mutation and four other mutations associated with cataract in humans are indicated. Mutations are numbered according to their amino-acid position in the processed CRYGD protein, which lacks an N-terminal methionine.

three other intervening markers, suggesting that the cataract locus lies in the 9.8 Mb physical interval, D2S1384-(2.2 Mb)-D2S369-(3.7 Mb)-D2S157-(1.2 Mb)-D2S371-(2.7 Mb)-D2S128, which spanned the γ-crystallin gene cluster (*CRYGA-CRYGF*), but excluded the gene for βA2-crystallin (*CRYBA2*).

Mutation analysis: Four functional candidate genes (*CRYGA-CRYGD*), and two pseudogenes (*CRYGE-F*) with in-frame translation stop codons, are clustered within the physical region defined for the cataract on 2q (Ensembl). We systematically sequenced all four functional *CRYG* genes, each comprising 3 exons and 2 introns (Figure 2D), in two affected and two unaffected members of the family using intron specific primers (Table 1). In addition to five single nucleotide polymorphisms (SNPs) referenced as rs796280, rs2854723, rs796287, rs2242074, rs2305430 in the NCBI SNP database, we detected a C->A transversion in exon 2 of *CRYGD* that

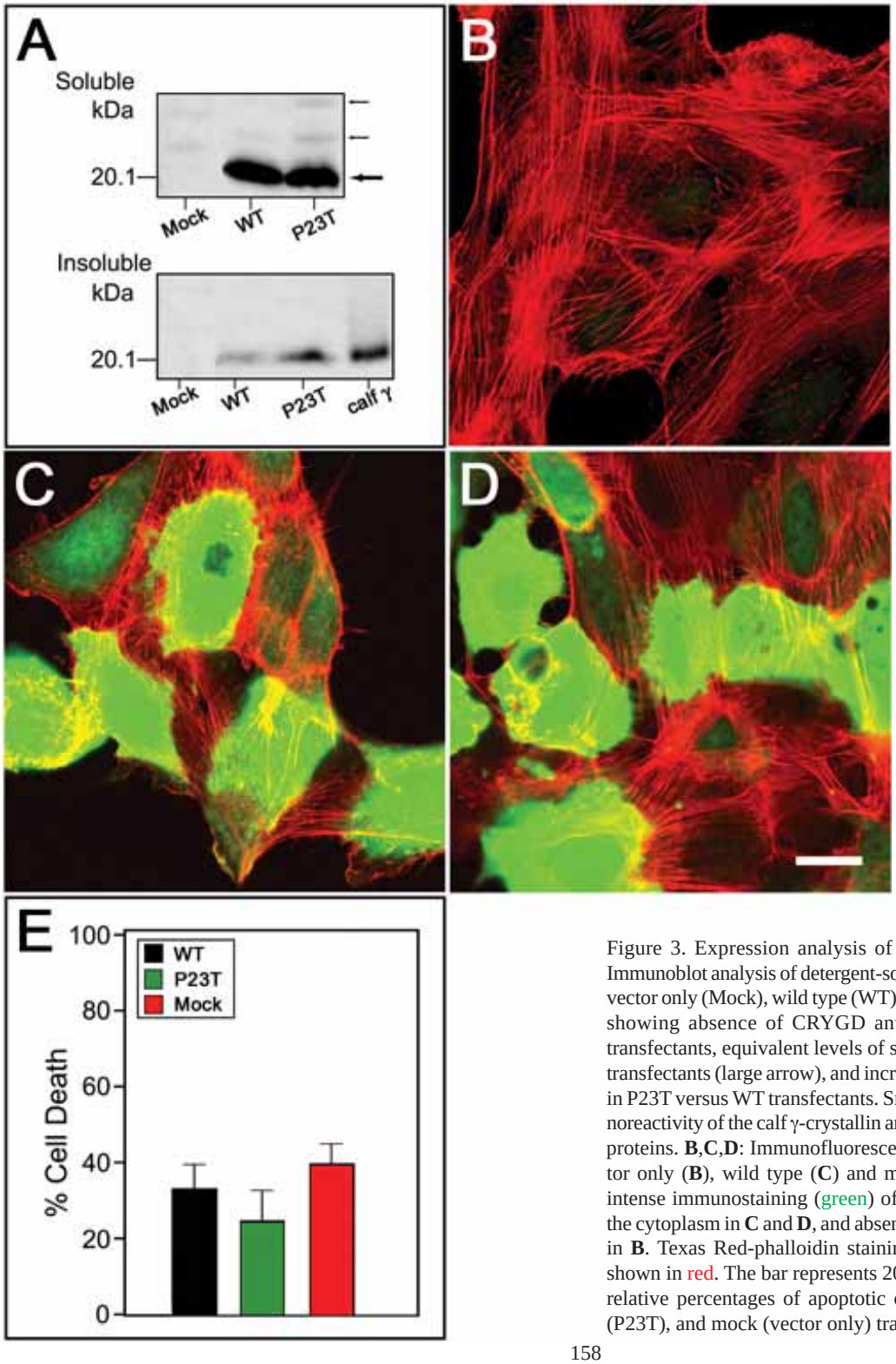

Figure 3. Expression analysis of CRYGD in HLE-B3 cells. **A**: Immunoblot analysis of detergent-soluble and insoluble fractions from vector only (Mock), wild type (WT), and mutant (P23T) transfectants, showing absence of CRYGD antigen (M_r 20.74 kDa) in Mock transfectants, equivalent levels of soluble CRYGD in WT and P23T transfectants (large arrow), and increased levels of insoluble CRYGD in P23T versus WT transfectants. Small arrows indicate weak immunoreactivity of the calf γ-crystallin antiserum with unidentified soluble proteins. **B**,**C**,**D**: Immunofluorescence confocal microscopy of vector only (**B**), wild type (**C**) and mutant (**D**) transfectants showing intense immunostaining (green) of CRYGD, primarily localized to the cytoplasm in **C** and **D**, and absence of significant immunostaining in **B**. Texas Red-phalloidin staining of the f-actin cytoskeleton is shown in red. The bar represents 20 μm. **E**: FACS analysis showing relative percentages of apoptotic cells in wild type (WT), mutant (P23T), and mock (vector only) transfectants.

was present in both of the affected individuals but not in either of the unaffected individuals (Figure 2A). As the C->A transversion did not result in the gain or loss of a convenient restriction site, we designed allele-specific primer extension analysis to confirm that the mutant "A" allele (Table 1) co-segregated with affected but not with unaffected members of the family (Figure 2C). Finally, we excluded the C->A transversion as a SNP in a panel of 170 normal unrelated individuals.

The C->A transversion occurred at the first base of codon 24, counting from the translation start (ATG) codon for methionine, and was predicted to result in a missense substitution of proline to threonine at amino-acid position 23 of the processed CRYGD protein, which lacks an N-terminal methionine (P23T). Alignment of the mammalian amino acid sequences for CRYGA-CRYGD present in the NCBI Protein Database, using the BLAST algorithm [39] revealed that either proline or serine, but never threonine, were conserved at amino-acid position 23. Although serine and threonine are both uncharged polar amino acids, the predicted P23T substitution represented a non-conservative amino-acid change, with the hydrophobic side-group of proline replaced by the polar (hydroxyl) side-group of threonine. Taken overall, the co-segregation of the C->A transition only with affected members of the pedigree and its absence in 340 normal chromosomes strongly suggested that the P23T substitution was a causative mutation rather than a benign SNP in linkage disequilibrium with the cataract.

Expression studies: In previous studies we have detected aberrant nuclear localization and cytotoxicity associated with a human αA-crystallin mutant when expressed in HLE B-3 cells [10]. In order to detect similar deleterious effects associated with the P23T substitution in CRYGD we transfected wild type and mutant *CRYGD* expression constructs into cultured HLE B-3 cells, which do not constitutively express significant levels of *CRYGD* transcript [40] or antigen (Figure 3A,B). Geneticin-resistant HLE-B3 transfectants that were expressing either wild type or mutant CRYGD at concentrations ranging between 0.5-2.0 ng/μg soluble protein, as determined by immunoblotting (Figure 3A), were selected for subsequent expression studies. Comparatively, the maximal levels of exogenous CRYGD attained in HLE B-3 transfectants (0.05-0.2% soluble protein) were 12-50 fold less than the endogenous levels of CRYGD (about 2.5% soluble protein) in the human fetal lens [1]. Clonal transfectants were used for up to four passages without detectable changes in the levels of exogenous wild type or mutant CRYGD as determined by immunoblot analysis. Whereas the levels of mutant and wild type CRYGD were similar in the soluble protein fraction, immunoblotting further indicated that the mutant was considerably more abundant than wild type in the insoluble membrane fraction (Figure 3A).

The sub-cellular distribution of wild type versus mutant CRYGD in HLE B-3 transfectants was compared using immunofluorescence confocal microscopy. Figure 3 shows that immunofluorescent labeling of wild type and mutant CRYGD was concentrated mainly in the cytoplasm surrounding the cell

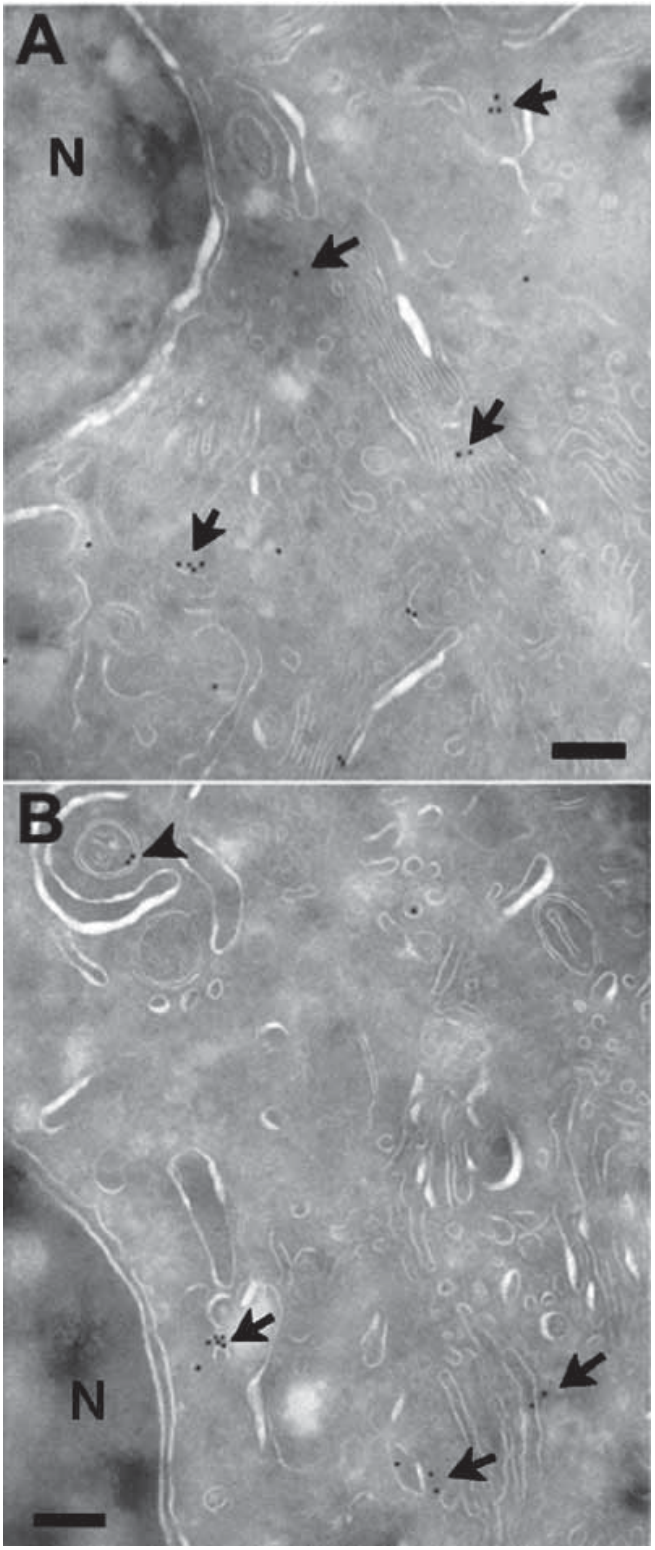

Figure 4. Ultrastructural localization of CRYGD in HLE B-3 cells. Cryo-immunoelectron microscopy of HLE B-3 cells expressing either wild type (**A**) or mutant (**B**) CRYGD showing that immuno-gold labeling (arrows in both panels) was primarily restricted to the cytoplasm. The arrowhead in **B** shows a double membrane structure surrounding immuno-gold particles. The letter N indicates the nucleus. The bar represents 1.5 μm. The magnification was x50,000.

nucleus; however, we could not exclude the possibility that some CRYGD was localized within cell nuclei, as reported for certain mouse γ-crystallins [41]. To further examine the sub-cellular localization of CRYGD at the ultrastructural level we used cryo-immunoelectron microscopy. Figure 4A shows that the immuno-gold labeling of wild type CRYGD was primarily localized to the cytoplasm, with no significant accumulation in cell nuclei. Similarly, immuno-gold labeling of mutant CRYGD was mainly cytoplasmic and occasionally appeared to be associated with single or double membrane structures (Figure 4B).

To compare the cytotoxic effects of mutant versus wild type CRYGD we measured the levels of apoptotic cell death in HLE B-3 transfectants. To quantify apoptosis, cells were incubated with annexin V (Ax), an inner plasma-membrane phospholipid binding protein, and propidium iodide (PI), a chromatin intercalating dye, and the percentage of labeled cells was determined by fluorescence-activated cell sorting (FACS) analysis (Figure 3E). Basal levels of cells that were in the early stages of apoptosis (Ax+/PI-) were similar in mock (vector only), wild type and mutant CRYGD transfectants indicating that the mutant was not significantly more cytotoxic than its wild type counterpart when expressed at the levels attained in HLE B-3 cells.

DISCUSSION

"Peculiar coralliform cataract", so named for the morphological resemblance of these lens opacities to sea coral, was first described in an individual in 1895 [36] and subsequently as an autosomal dominant trait in three English pedigrees circa 1910 [37,38]. Here, we have identified a missense substitution (P23T) in processed CRYGD that co-segregated with autosomal dominant coral-like cataract in a three-generation Caucasian family. During the course of this study, the same P23T substitution was independently associated with congenital lamellar cataract in a father and daughter of Indian descent [22], congenital cerulean cataract in a five-generation Morroccan family [26,27], and flaky, silica-like nuclear cataract in a five-generation Australian family [15]. Lamellar and cerulean forms of cataract are generally regarded as morphologically distinct types of lens opacities [7,8], with the former affecting a discrete opacified shell within an otherwise clear lens, whereas, the latter is characterized by blue-white dots in the outer nucleus progressing to wedge-shaped opacities in the cortex. No clinical photographs of the flaky, silica-like nuclear cataract were published [15], however, close inspection of the photographs of lamellar cataract in a three year old patient [22] and cerulean cataract in thirty-five and forty-five year old patients [26] does reveal striking resemblances to the original drawing of coralliform cataract in a twenty-two year old patient published in 1895 [36].

In addition to the P23T substitution, three other missense substitutions and one nonsense termination in *CRYGD* have been associated with cataract, including aculeiform (needle-like crystals) cataract (R58H) in Macedonian and Swiss families [20,23], progressive pulverulent (punctate) cataract (R14C) in an American family [25], crystal-related cataract [R36S] in a five year old Czech boy [24], and central nuclear cataract (W156X) in a father and daughter of Indian descent [22]. Thus, like the cerulean, coralliform, and flaky opacities associated with the P23T substitution, these other *CRYGD*-related opacities involve the central nucleus of the lens and may also progressively affect the outer cortex.

Based on the crystal structure of human CRYGD, the P23T substitution lies in the N-terminal domain within the first Greek-key motif [42]. Molecular modeling data [27] has indicated that proline 23 interacts with asparigine 49 in wild type CRYGD, whereas, threonine 23 interacts with asparigine 49 and tyrosine 50 in mutant CRYGD. However, the deleterious effects of threonine 23 on CRYGD folding, stability, and solubility are unclear especially when serine, which is structurally similar to threonine, can replace proline 23 as the wild type in other species. Interestingly, biophysical studies of three other CRYGD missense substitutions (R14C, R36S, R58H) have detected deleterious gain-of-function effects, which manifest as insolubility and/or crystal nucleation in the absence of significant protein conformational changes. Thus, the R14C mutant, associated with progressive punctuate cataract, forms disulfide-linked oligomers in vitro culminating in aggregation of this normally monomeric protein [43], whereas, the R36S and R58H mutants, associated with crystal-like and aculeiform cataract, respectively, promote deposition of CRYGD-protein crystals in vitro [42,44] and in the lens [20,23,24]. Remarkably, iridescent crystals were also observed throughout the clearer part of the lens in the original 1895 description of coralliform cataract [36]. Although we did not observe crystal-formation by the recombinant P23T mutant when expressed in cultured HLE B-3 cells, possibly as a result of the relatively low level of CRYGD protein compared with that in the lens, there was evidence of membrane-associated insolubility. Biophysical studies of the P23T mutant, and others (e.g., P23S), will be required to provide further insights regarding the molecular pathology of CRYGD-related cataract.

Finally, it is noteworthy that an autosomal dominant coralliform cataract mutation (*Coc*) has also been reported in the mouse [45]. Although no *Coc* mouse lens photographs were published the cataract was described as having small, round irregularly shaped opacities resembling corals located in the fetal nucleus. Thus, despite the significant morphological differences between mouse and human lenses the coralliform phenotype appears remarkably consistent. The *Coc* locus has been linked to a region of murine chromosome 16 with conserved synteny to a region of human chromosome 3 [46]. Interestingly, this linkage excluded as causative the murine γ-crystallin gene cluster (*Cryga-Crygf*), which maps to chromosome 1. In addition, the murine γS-crystallin gene (*Crygs*), which harbors the opacity due to poor secondary fiber junctions (*Opj*) mutation [47] located about 20 centi-Morgans proximal to *Coc* on chromosome 16, was also excluded as causative [46]. Identification of the *Coc* gene will provide novel insights regarding coralliform cataract in mice and raises the possibility of genetic heterogeneity for this peculiar type of hereditary cataract in humans.

ACKNOWLEDGEMENTS

We thank the family for participating in this study, Dr. O Boskovska for help with ascertaining the family, J-H Xi and F Bai for excellent technical assistance, and C. Shomo for help with graphics. This work is supported by NIH/NEI grants EY12284 (AS), EY05681 (UPA), EY02687 and Research to Prevent Blindness (RPB). UPA is a recipient of the Lew R. Wasserman award from RPB.

REFERENCES

1. Lampi KJ, Ma Z, Shih M, Shearer TR, Smith JB, Smith DL, David LL. Sequence analysis of betaA3, betaB3, and betaA4 crystallins completes the identification of the major proteins in young human lens. J Biol Chem 1997; 272:2268-75.
2. Bhat SP. Crystallins, genes and cataract. Prog Drug Res 2003; 60:205-62.
3. Delaye M, Tardieu A. Short-range order of crystallin proteins accounts for eye lens transparency. Nature 1983; 302:415-7.
4. Fernald RD, Wright SE. Maintenance of optical quality during crystalline lens growth. Nature 1983; 301:618-20.
5. Fernald RD, Wright SE. Optical quality during crystalline lens growth. Nature 1984; 312:292.
6. Rahi JS, Dezateaux C, British Congenital Cataract Interest Group. Measuring and interpreting the incidence of congenital ocular anomalies: lessons from a national study of congenital cataract in the UK. Invest Ophthalmol Vis Sci 2001; 42:1444-8.
7. Brown N. A. Phelps, Bron AJ. Lens Disorders: a clinical manual of cataract diagnosis. Oxford, UK: Butterworth-Heineman Ltd.; 1995.
8. Ionides A, Francis P, Berry V, Mackay D, Bhattacharya S, Shiels A, Moore A. Clinical and genetic heterogeneity in autosomal dominant cataract. Br J Ophthalmol 1999; 83:802-8.
9. Litt M, Kramer P, LaMorticella DM, Murphey W, Lovrien EW, Weleber RG. Autosomal dominant congenital cataract associated with a missense mutation in the human alpha crystallin gene CRYAA. Hum Mol Genet 1998; 7:471-4.
10. Mackay DS, Andley UP, Shiels A. Cell death triggered by a novel mutation in the alphaA-crystallin gene underlies autosomal dominant cataract linked to chromosome 21q. Eur J Hum Genet 2003; 11:784-93.
11. Pras E, Frydman M, Levy-Nissenbaum E, Bakhan T, Raz J, Assia EI, Goldman B, Pras E. A nonsense mutation (W9X) in CRYAA causes autosomal recessive cataract in an inbred Jewish Persian family. Invest Ophthalmol Vis Sci 2000; 41:3511-5.
12. Berry V, Francis P, Reddy MA, Collyer D, Vithana E, MacKay I, Dawson G, Carey AH, Moore A, Bhattacharya SS, Quinlan RA. Alpha-B crystallin gene (CRYAB) mutation causes dominant congenital posterior polar cataract in humans. Am J Hum Genet 2001; 69:1141-5.
13. Kannabiran C, Rogan PK, Olmos L, Basti S, Rao GN, Kaiser-Kupfer M, Hejtmancik JF. Autosomal dominant zonular cataract with sutural opacities is associated with a splice mutation in the betaA3/A1-crystallin gene. Mol Vis 1998; 4:21 .
14. Bateman JB, Geyer DD, Flodman P, Johannes M, Sikela J, Walter N, Moreira AT, Clancy K, Spence MA. A new betaA1-crystallin splice junction mutation in autosomal dominant cataract. Invest Ophthalmol Vis Sci 2000; 41:3278-85.
15. Burdon KP, Wirth MG, Mackey DA, Russell-Eggitt IM, Craig JE, Elder JE, Dickinson JL, Sale MM. Investigation of crystallin genes in familial cataract, and report of two disease associated mutations. Br J Ophthalmol 2004; 88:79-83.
16. Gill D, Klose R, Munier FL, McFadden M, Priston M, Billingsley G, Ducrey N, Schorderet DF, Heon E. Genetic heterogeneity of the Coppock-like cataract: a mutation in CRYBB2 on chromosome 22q11.2. Invest Ophthalmol Vis Sci 2000; 41:159-65.
17. Mackay DS, Boskovska OB, Knopf HL, Lampi KJ, Shiels A. A nonsense mutation in CRYBB1 associated with autosomal dominant cataract linked to human chromosome 22q. Am J Hum Genet 2002; 71:1216-21.
18. Litt M, Carrero-Valenzuela R, LaMorticella DM, Schultz DW, Mitchell TN, Kramer P, Maumenee IH. Autosomal dominant cerulean cataract is associated with a chain termination mutation in the human beta-crystallin gene CRYBB2. Hum Mol Genet 1997; 6:665-8.
19. Vanita Sarhadi V, Reis A, Jung M, Singh D, Sperling K, Singh JR, Burger J. A unique form of autosomal dominant cataract explained by gene conversion between beta-crystallin B2 and its pseudogene. J Med Genet 2001; 38:392-6.
20. Heon E, Priston M, Schorderet DF, Billingsley GD, Girard PO, Lubsen N, Munier FL. The gamma-crystallins and human cataracts: a puzzle made clearer. Am J Hum Genet 1999; 65:1261-7.
21. Ren Z, Li A, Shastry BS, Padma T, Ayyagari R, Scott MH, Parks MM, Kaiser-Kupfer MI, Hejtmancik JF. A 5-base insertion in the gammaC-crystallin gene is associated with autosomal dominant variable zonular pulverulent cataract. Hum Genet 2000; 106:531-7.
22. Santhiya ST, Shyam Manohar M, Rawlley D, Vijayalakshmi P, Namperumalsamy P, Gopinath PM, Loster J, Graw J. Novel mutations in the gamma-crystallin genes cause autosomal dominant congenital cataracts. J Med Genet 2002; 39:352-8.
23. Heon E, Liu S, Billingsley G, Bernasconi O, Tsilfidis C, Schorderet DF, Munier FL, Tsifildis C. Gene localization for aculeiform cataract, on chromosome 2q33-35. Am J Hum Genet 1998; 63:921-6. Erratum in: Am J Hum Genet 1999 Jan; 64(1):334.
24. Kmoch S, Brynda J, Asfaw B, Bezouska K, Novak P, Rezacova P, Ondrova L, Filipec M, Sedlacek J, Elleder M. Link between a novel human gammaD-crystallin allele and a unique cataract phenotype explained by protein crystallography. Hum Mol Genet 2000; 9:1779-86.
25. Stephan DA, Gillanders E, Vanderveen D, Freas-Lutz D, Wistow G, Baxevanis AD, Robbins CM, VanAuken A, Quesenberry MI, Bailey-Wilson J, Juo SH, Trent JM, Smith L, Brownstein MJ. Progressive juvenile-onset punctate cataracts caused by mutation of the gammaD-crystallin gene. Proc Natl Acad Sci U S A 1999; 96:1008-12.
26. Hilal L, Nandrot E, Belmekki M, Chefchaouni M, El Bacha S, Benazzouz B, Hajaji Y, Gribouval O, Dufier J, Abitbol M, Berraho A. Evidence of clinical and genetic heterogeneity in autosomal dominant congenital cerulean cataracts. Ophthalmic Genet 2002; 23:199-208.
27. Nandrot E, Slingsby C, Basak A, Cherif-Chefchaouni M, Benazzouz B, Hajaji Y, Boutayeb S, Gribouval O, Arbogast L, Berraho A, Abitbol M, Hilal L. Gamma-D crystallin gene (CRYGD) mutation causes autosomal dominant congenital cerulean cataracts. J Med Genet 2003; 40:262-7.
28. Dib C, Faure S, Fizames C, Samson D, Drouot N, Vignal A, Millasseau P, Marc S, Hazan J, Seboun E, Lathrop M, Gyapay G, Morissette J, Weissenbach J. A comprehensive genetic map of the human genome based on 5,264 microsatellites. Nature 1996; 380:152-4.
29. Lathrop GM, Lalouel JM, Julier C, Ott J. Strategies for multilocus linkage analysis in humans. Proc Natl Acad Sci U S A 1984; 81:3443-6.

30. Collins JS, Schwartz CE. Detecting polymorphisms and mutations in candidate genes. Am J Hum Genet 2002; 71:1251-2.
31. Andley UP, Rhim JS, Chylack LT Jr, Fleming TP. Propagation and immortalization of human lens epithelial cells in culture. Invest Ophthalmol Vis Sci 1994; 35:3094-102.
32. Andley UP, Song Z, Wawrousek EF, Bassnett S. The molecular chaperone alphaA-crystallin enhances lens epithelial cell growth and resistance to UVA stress. J Biol Chem 1998; 273:31252-61.
33. Andley UP, Song Z, Wawrousek EF, Fleming TP, Bassnett S. Differential protective activity of alpha A- and alphaB-crystallin in lens epithelial cells. J Biol Chem 2000; 275:36823-31.
34. Bai F, Xi JH, Wawrousek EF, Fleming TP, Andley UP. Hyperproliferation and p53 status of lens epithelial cells derived from alphaB-crystallin knockout mice. J Biol Chem 2003; 278:36876-86.
35. Hay RE, Andley UP, Petrash JM. Expression of recombinant bovine gamma B-, gamma C- and gamma D-crystallins and correlation with native proteins. Exp Eye Res 1994; 58:573-84.
36. Gunn RM. Peculiar coralliform cataract with crystals in the lens. Transactions of the Ophthalmological Society of the United Kingdom (London) 1895; XV:119.
37. Nettleship E. Seven new pedigrees of hereditary cataract. Trans Ophthalmol Soc U K 1909; 29:188-211.
38. Harman NB. Ten pedigrees of congenital and infantile cataract; lamellar, coralliform, discoid, and posterior polar with microphthalmia. Trans Ophthalmol Soc U K 1910; 30:251-274.
39. Altschul SF, Gish W, Miller W, Myers EW, Lipman DJ. Basic local alignment search tool. J Mol Biol 1990; 215:403-10.
40. Fleming TP, Song Z, Andley UP. Expression of growth control and differentiation genes in human lens epithelial cells with extended life span. Invest Ophthalmol Vis Sci 1998; 39:1387-98.
41. Sandilands A, Hutcheson AM, Long HA, Prescott AR, Vrensen G, Loster J, Klopp N, Lutz RB, Graw J, Masaki S, Dobson CM, MacPhee CE, Quinlan RA. Altered aggregation properties of mutant gamma-crystallins cause inherited cataract. EMBO J 2002; 21:6005-14.
42. Basak A, Bateman O, Slingsby C, Pande A, Asherie N, Ogun O, Benedek GB, Pande J. High-resolution X-ray crystal structures of human gammaD crystallin (1.25 A) and the R58H mutant (1.15 A) associated with aculeiform cataract. J Mol Biol 2003; 328:1137-47.
43. Pande A, Pande J, Asherie N, Lomakin A, Ogun O, King JA, Lubsen NH, Walton D, Benedek GB. Molecular basis of a progressive juvenile-onset hereditary cataract. Proc Natl Acad Sci U S A 2000; 97:1993-8.
44. Pande A, Pande J, Asherie N, Lomakin A, Ogun O, King J, Benedek GB. Crystal cataracts: human genetic cataract caused by protein crystallization. Proc Natl Acad Sci U S A 2001; 98:6116-20.
45. Kratochvilova J, Favor J. Phenotypic characterization and genetic analysis of twenty dominant cataract mutations detected in offspring of irradiated male mice. Genet Res 1988; 52:125-34.
46. Sidjanin DJ, Grimes PA, Pretsch W, Neuhauser-Klaus A, Favor J, Stambolian DE. Mapping of the autosomal dominant cataract mutation (Coc) on mouse chromosome 16. Invest Ophthalmol Vis Sci 1997; 38:2502-7.
47. Sinha D, Wyatt MK, Sarra R, Jaworski C, Slingsby C, Thaung C, Pannell L, Robison WG, Favor J, Lyon M, Wistow G. A temperature-sensitive mutation of Crygs in the murine Opj cataract. J Biol Chem 2001; 276:9308-15.

The print version of this article was created on 17 Mar 2004. This reflects all typographical corrections and errata to the article through that date. Details of any changes may be found in the online version of the article.